Nitrogen and Proton ENDOR of Cytochrome *d*, Hemin, and Metmyoglobin in Frozen Solutions

Fa. S. Jiang,[§,†] Tamma M. Zuberi,[⊥] Jeffrey B. Cornelius,[∥,‡] R. B. Clarkson,[∥,#] Robert B. Gennis,[⊥] and R. L. Belford*[,§,∥]

Contribution from the Departments of Chemistry and Biochemistry, School of Chemical Sciences, Illinois EPR Research Center, and Department of Veterinary Clinical Medicine, University of Illinois, 505 South Mathews Avenue, Urbana, Illinois 61801

Received January 27, 1992

Abstract: Orientation-selected electron nuclear double resonance (ENDOR) spectra have been obtained from iron-linked nitrogens of the *d* heme of the cytochrome *d* oxidase complex in frozen solution. Heme *d* is a high-spin chlorin moiety which exists in the cytochrome *d* complex located in the inner membrane of *Escherichia coli*. This complex is a terminal oxidase in the *E. coli* aerobic respiratory chain. Comparison of the spectra of cytochrome *d* with hemin and metmyoglobin strongly implies that the *d* heme does not contain an axial nitrogen ligand. By computer simulation of the ENDOR spectra for each magnetic field, the nitrogen hyperfine interaction matrices and quadrupole coupling tensors to the three heme groups were determined. For each of the three heme groups studied, the proton hyperfine coupling perpendicular to the heme plane was also measured. From average hyperfine coupling constants, the unpaired electron densities in the nitrogen 2s and 2p valence orbitals were calculated with standard ligand field techniques. The quadrupole constants are also related to electron populations in the nitrogen orbitals. The comparison between theoretical calculations and experimental data is shown.

Introduction

Cytochrome *d* is a high-spin chlorin which exists in the cytochrome *d* oxidase complex in the inner membrane of *Escherichia coli*. The aerobic respiratory chain of *E. coli* has no cytochrome *c* and no equivalent to the mitochondrial Complex III (bc_1 complex) or Complex IV (cytochrome *c* oxidase). Instead, two terminal oxidases, the cytochrome *o* and cytochrome *d* complexes, expressed at different stages of cell growth, can oxidize ubiquinol directly and reduce molecular oxygen to water, concomitantly generating an electrochemical proton gradient across the membrane.[1]

The cytochrome *d* oxidase complex contains three heme groups: b_{558}, b_{595}, and *d*. Site-directed mutagenesis has been performed on the histidines of the complex to determine possible heme ligands, and two mutants were isolated that are of particular interest.[2] Mutations of histidine to leucine at positions 19 and 186 of subunit I affect heme binding, although both subunits of the complex are expressed and intact. Mutations in histidine 186 result in loss of the b_{558} heme, although b_{595} and *d* are still bound. This strongly suggests that histidine 186 acts as one axial ligand to the hexacoordinate b_{558}. Mutations in histidine 19, however, result in loss of both b_{595} and *d* but leave b_{558} bound. Therefore it is possible that this residue acts as either the ligand to b_{595}, as the ligand to *d*, or as an important residue in the structural integrity of the b_{595}–*d* active site. Our goal in this work was to determine if the *d* heme does indeed have a histidine proximal ligand through the use of ENDOR, thereby obtaining increased evidence to either support or reject the idea of histidine 19 as an axial ligand to this heme group.

The electron spin of transition-metal ions and free radicals interacts with the nuclear spin of nuclei that surround the unpaired electron so that shifts in the NMR lines of the nuclei are observed. Since NMR spectroscopy of paramagnetic samples has limited sensitivity and low selectivity, the extraction of structure and hyperfine parameters can be difficult using this technique. Electron nuclear double resonance (ENDOR) has been used as an alternative technique[3-7] to determine the nature of nuclei surrounding the paramagnetic ion and to determine the hyperfine coupling constants. When the spin–lattice relaxation time, T_{1e}, is much less than the intersite cross relaxation time, T_x, a single-crystal-like ENDOR spectrum can be observed at a turning point in the powder EPR spectrum. At other regions, complicated ENDOR spectra will be obtained.[6,7] In this case, a quantitative treatment of angle-selected ENDOR spectra can be done.[8] When $T_x \ll T_{1e}$, no matter which portion of the EPR lines is saturated, the ENDOR spectrum is the same and is the sum of all the possible ENDOR lines. This case was discussed by Kwiram and co-workers.[4,5] In magnetically dilute systems with very large anisotropy (wide separation of turning points), one expects to observe the single-crystal-like spectra. The systems described here belong to this case.

Previous ENDOR on high-spin ferric heme and heme proteins has been reported on frozen solutions[9,10] or single-crystal samples.[11] Single-crystal-like ENDOR spectra of protoporphyrin and histidine ligand nitrogens of metmyoglobin were reported from frozen solution samples at the $g_z = 2.00$ extreme, corresponding to the normal of the heme plane. However, ENDOR spectra at other EPR line positions were not reported, and the complete nitrogen hyperfine coupling tensor thus could not be obtained from the

* To whom correspondence may be addressed. Telephone: (217) 333-2553.
† Present Address: Department of Biochemistry and Molecular Biology, University of Chicago, 920 E. 58th St., Chicago, IL 60637.
‡ Present Address: Principia College, Elsah, IL 62028.
§ Department of Chemistry, University of Illinois.
⊥ Department of Biochemistry, University of Illinois.
∥ School of Chemical Sciences, Illinois EPR Research Center, University of Illinois.
Department of Veterinary Clinical Medicine, University of Illinois.

(1) Anraku, Y.; Gennis, R. B. *TIBS* **1987**, *12*, 262–266.
(2) Fang, H.; Lin, R.-J.; Gennis, R. B. *J. Biol. Chem.* **1989**, *264*, 8026–8032.
(3) Feher, G. *Phys. Rev.* **1956**, *103*, 834–835.
(4) Kwiram, A. L. *J. Chem. Phys.* **1968**, *49*, 2860–2861.
(5) Dalton, L. R.; Kwiram, A. L. *J. Chem. Phys.* **1972**, *57*, 1132–1145.
(6) Rist, G. H.; Hyde, J. S. *J. Chem. Phys.* **1968**, *49*, 2449–2451.
(7) Rist, G. H.; Hyde, J. S. *J. Chem. Phys.* **1970**, *52*, 4633–4643.
(8) Henderson, T. A.; Hurst, G. C.; Kreilick, R. W. *J. Am. Chem. Soc.* **1985**, *107*, 7299–7303.
(9) Scholes, C. P.; Isaacson, R. A.; Feher, G. *Biochim. Biophys. Acta* **1972**, *263*, 448–452.
(10) Feher, G.; Isaacson, R. A.; Scholes, C. P.; Nagel, R. *Ann. N.Y. Acad. Sci.* **1973**, *222*, 86–101.
(11) Scholes, C. P.; Lapidot, A.; Mascarenhas, R.; Inubushi, T.; Issacson, R. A.; Feher, G. *J. Am. Chem. Soc.* **1982**, *104*, 2724–2735.

0002-7863/93/1515-10293$04.00/0

frozen solution samples. The single-crystal ENDOR study of aquometmyoglobin by Scholes *et al.*[11] is a tour de force which provides valuable benchmarks for assessing angle-selected powder ENDOR.

This work contains the first report of the nitrogen and proton ENDOR spectra of cytochrome *d*. The nitrogen hyperfine coupling tensors of cytochrome *d* were obtained from simulations by a computer program, NANGSEL, written by one of us (J.B.C.; see Acknowledgments). Also, for comparison purposes, nitrogen and proton ENDOR spectra of frozen solutions of aquometmyoglobin and hydroxylhemin were examined in the same way.

Spin Hamiltonian

For the overall ferric ground state ($S = {}^5/_2$) sextet, the spin Hamiltonian for analyzing EPR and ENDOR spectra has the form

$$\mathcal{H}_{spin} = \beta_e \mathbf{BgS} + \mathbf{SDS} + h\mathbf{SA}_{Fe}\mathbf{I}_{Fe} - g_{Fe}\beta_N \mathbf{BI}_{Fe} + \sum_L h(\mathbf{SA}_L + \mathbf{I}_L\mathbf{P}_L - g_L\beta_N\mathbf{B})\mathbf{I}_L \quad (1)$$

where **B** is the applied magnetic field, **S** is the electron spin, $\mathbf{I}_{Fe}$ is the iron nuclear spin, β_e and β_N are the electronic and nuclear Bohr magnetons, respectively, and L is a ligand nucleus. **D** represents the zero-field splitting (the electronic quadrupole term), **P** the nuclear quadrupole coupling matrix, and $\mathbf{A}_{Fe}$ the hyperfine coupling of the central iron ion with the electron spin. The summation over ligand nuclei includes the four pyrrole nitrogen atoms, the histidine nitrogen (assuming a histidine axial ligand), and the protons. The three terms bracketed within the summation described the ligand nuclear hyperfine, the ligand nuclear electric quadrupole, and the ligand nuclear Zeeman interactions for nucleus L. However, since the zero-field splitting is much larger than the electronic Zeeman splitting, EPR and ENDOR spectra ordinarily are observed only from the ground $M_S = \pm{}^1/_2$ doublet of the sextet. Since the natural abundance of ^{57}Fe is small, the Hamiltonian for ligand ENDOR becomes[11]

$$\mathcal{H}_{eff} = \sum_L (h\mathbf{S}'\mathbf{A}'_L + \mathbf{I}_L\mathbf{P}_L - \beta_N\mathbf{B}g_L)\mathbf{I}_L \quad (2)$$

where **S**′ is an effective ($S' = {}^1/_2$) electron spin vector for the $M_S = \pm{}^1/_2$ submanifold and $\mathbf{A}'_L$ is the corresponding effective ligand hyperfine coupling matrix. The relationship between $\mathbf{A}'_L$ and $\mathbf{A}_L$ is

$$\mathbf{A}'_L = \mathbf{g}_{eff}\mathbf{g}^{-1}\mathbf{A}_L \quad (2a)$$

where $\mathbf{g}_{eff}$ is the effective **g** matrix for the $S' = {}^1/_2$ description. Since the true **g** matrix in this *S*-state ion is nearly isotropic with a value of 2.00, we have

$$\mathbf{A}'_L \approx \mathbf{g}_{eff}\mathbf{A}_L/2 \quad (2b)$$

Finally, since $\mathbf{g}_{eff}$ here is essentially axial, with $g_{eff,z} = 2.00$ and $g_{eff,x,y} = 5.94$ (see below) and since each $\mathbf{A}_L$ ought to have one canonical axis essentially normal to the heme plane (i.e., *z*), we have

$$A'_{Lz} \approx A_{Lz}; \quad A'_{Lx} \approx 2.97\,A_{Lx}; \quad A'_{Ly} \approx 2.97\,A_{Ly} \quad (2c)$$

There will be an unusually large "pseudonuclear" contribution to the apparent nitrogen nuclear **g** tensor. The last term in eq 2 for any ligand nitrogen becomes[11]

$$\beta_N\mathbf{B}g_L\mathbf{I}_L = g_{Nx}\beta_N\mathbf{B}\sin\theta(\cos\phi\cos\alpha - \sin\phi\sin\alpha)I_x - g_{Ny}\beta_N\mathbf{B}\sin\theta(\cos\phi\sin\alpha + \sin\phi\cos\alpha)I_y - g_{Nz}\beta_N\mathbf{B}\cos\theta I_z \quad (3)$$

where θ and ϕ are the polar and azimuthal angles which the applied magnetic field makes with respect to the **g**-tensor axes *x*, *y*, and *z*, and α is the angle between the g_x vector and the nitrogen hyperfine coupling A_{Nx} vector. Additional formulas which were used in the calculations and in the simulation program are listed in the Appendix.

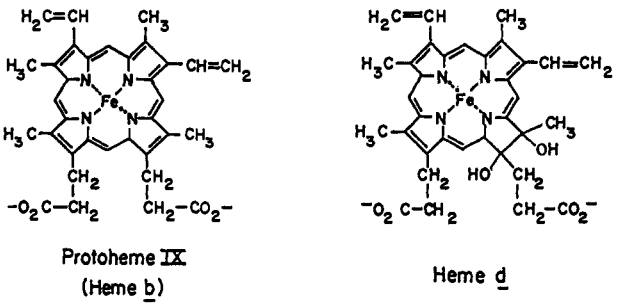

Figure 1. Structures of the heme moieties studied. (a) Protoporphyrin IX of hemin and metmyoglobin. (b) Heme *d* as proposed by Timkovich.[24] The axial ligands of the ferric ion in the heme groups are not shown.

Materials and Methods

Materials. Sodium cholate, sodium *N*-lauroylsarcosine, and (phenylmethyl)sulfonyl fluoride (PMSF) were purchased from Sigma Chemical Corp. *N*-Dodecyl *N*,*N*-dimethylammonium-3-propanesulfonate (sulfobetaine 12, or SB-12) was purchased from Serva Biochemicals. Leupeptin was obtained from Boehringer Mannheim.

The cytochrome *d* oxidase complex was isolated from *E. coli* as described by Miller and Gennis.[12] As isolated, the cytochrome *d* complex is in an inactive state in the detergent cholate. It may be reactivated by exchanging the detergent cholate for another detergent such as sarcosyl. Cholate was exchanged for sarcosyl by dialysis in 10 mM sodium phosphate, 5 mM EDTA, and 0.025% sarcosyl, pH 8.0. PMSF and leupeptin were added to the dialysis buffers to prevent proteolysis. A small amount of ferricyanide was also added to the final dialysis buffer to fully oxidize the isolated protein. The complex was concentrated using the Amicon ultrafiltration system with a PM30 membrane. The final concentration of the complex used in these studies was 283 μM.

Hemin chloride (bovine, Type I) was purchased from Sigma. A 3 mM hemin solution was made in dimethylformamide–methanol (1:1, v/v). In this solution the majority of the hemin would be expected to be in the hydroxyl-bound form.

Horse skeletal muscle myoglobin was purchased from ICN Biomedicals and was used without further purification. Six-millimolar samples were prepared in a 50% (v/v) glycerol, 0.1 M potassium phosphate buffer (pH 6.0). In this buffer at pH 6.0, the metmyoglobin is expected to have a water bound at the sixth coordination site. Figure 1 shows the chemical structures of hemin and the *d* heme.

D_2O for deuteration experiments was purchased from Sigma in 99.9 atom % D. Deuterated samples of cytochrome *d* oxidase were produced by several dilutions of the protein into deuterated buffer followed by concentration with an Amicon filtration device.

EPR/ENDOR Spectrometer. X-band EPR spectra were obtained on a Varian E-12 EPR spectrometer. A Varian NMR gaussmeter, 92980/02P, was used for magnetic field measurements. A Fluke 1910A Multi-Counter with a Hewlett–Packard 5260A frequency divider was applied to measure the EPR frequency.

The ENDOR spectra were run on a Varian E-12 X-band spectrometer equipped with an ENDOR control, Varian E-1700 ENDOR system, the FM modulation module previously described,[13] and an IBM PC signal averager. A version of the EW software package (Scientific Software Systems, Bloomington, IL) was used for the spectrometer control and data collection. A 12.5-kHz FM modulation of the radiofrequency (rf) field was applied with a modulation amplitude (Δf) of between 100 and 200 kHz to ensure maximum ENDOR signals without serious line broadening. Field modulation was not used. The modulated radiofrequency was amplified by an ENI Model 3200L power amplifier and driven through the ENDOR coil. Typically, a range of 25 MHz was swept in 30 s, and the resultant ENDOR RF-induced signal was collected in the PC signal averager. The temperature was controlled by an Air Products liquid helium variable temperature system. The experiments were performed at 7 K.

(12) Miller, M. J.; Gennis, R. B. *J. Biol. Chem.* **1983**, *258*, 9159–9165.
(13) Clarkson, R. B.; Belford, R. L.; Reiner, C. *Rev. Sci. Instrum.* **1990**, *61*, 3356–3359.

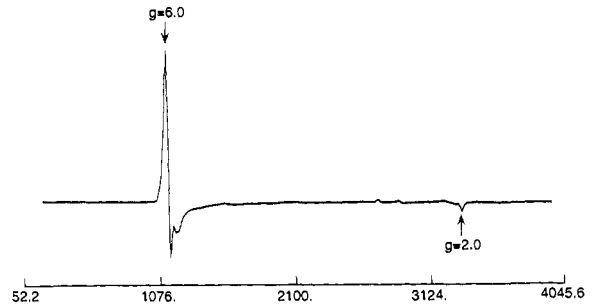

Figure 2. EPR spectrum of isolated cytochrome *d* complex from the membranes of *E. coli*. EPR conditions: microwave power, 2 mW; modulation frequency, 100 kHz; modulation amplitude, 2 G; scan time, 2 min; time constant, 0.25 s; temperature, 7 K, microwave frequency, 9.3242 GHz. Ordinate: first derivative of absorption with respect to field intensity. Abscissa: magnetic field intensity **B**, in gauss = 10^{-4} tesla.

N-14 ENDOR Simulation. The complexity of the powder ENDOR spectra requires computer simulation to yield accurate parameters for the ligand hyperfine coupling tensors. The method employed is based on the approach of Hurst, Henderson, and Kreilick.[8] In this approach, the electron Zeeman interaction is taken as the dominant energy term, so that the coordinate system where the **g** tensor is diagonal is chosen as the frame of reference. Given a specific orientation, an effective electron-nuclear distance, A_{Fermi}, and a nuclear **g** value, the program NANGSEL computes nitrogen anisotropic hyperfine coupling matrices by using eq 2′ in the Appendix. The nitrogen nuclear quadrupole coupling also is included. In the powder or frozen solution, a uniform distribution of molecular orientations is assumed. Each applied field value at resonance selects a specific set of these molecular orientations which contribute to the ENDOR spectrum. The program calculates the ENDOR transition frequencies at each molecular orientation selected. Results of nitrogen hyperfine coupling are then summed over all the selected orientations to produce a composite stick spectrum on a discrete radiofrequency grid. After convoluting with a line width function, an absorption ENDOR spectrum is calculated and finally displayed in derivative mode.

The program requires the user to specify three things: (1) the magnetic field used in the experiment, (2) the angular intervals $\Delta\theta$ and $\Delta\phi$ to be used in the summation over orientations, and (3) the number of nitrogen nuclei that have the same spin but different magnetic moments and orientations. For each unique nucleus, one specifies the principal values of the hyperfine coupling matrix (or the orientations of the hyperfine coupling in the **g** axis system and the distance between the center iron ion and the nitrogen atom) and the nuclear quadrupole tensor. As mentioned above, the apparent nuclear $\mathbf{g}_N$ values of the nitrogens are anisotropic. However, in the program the $\mathbf{g}_N$ values are treated as isotropic. If the spectrum is from the **g** = 2.00 region, then the g_{Nz} of the nitrogen nucleus is 0.4037, and the g_{Nx} and g_{Ny} will not affect the ENDOR spectrum. If it is from the **g** = 5.94 region, the average value of g_{Nx} and g_{Ny} of the nitrogen nucleus is used. This approximation is adequate for obtaining the parameters since the difference between the g_{Nx} (0.61) and g_{Ny} (0.54) is small and the contribution of g_{Nz} to the ENDOR spectra at the **g** = 5.94 region can be ignored. The information presented in this paper was obtained from computer simulations done in the two regions mentioned above, namely, the **g** = 2.0 and **g** = 5.94 regions. In the simulation, variables were adjusted until the best fit for the spectrum at each specific magnetic field had been obtained; optimization of the simulations was based on ENDOR peak positions, and intensities were not explicitly considered in the fitting of experimental and simulated spectra (see below).

Results

EPR Spectrum of the Cytochrome *d* Complex. Figure 2 shows an X-band EPR spectrum of the cytochrome *d* complex in frozen solution at 7 K. The axial signal, $g_{\parallel} = 2$, $g_{\perp} = 6$, resembles the spectrum of metmyoglobin[10] which contains a high-spin protoporphyrin IX heme group. This signal ($g = 2.0, 5.94$) has been assigned to the *d* heme in the cytochrome *d* complex.[14] The lines at 6.26 and 5.55 are assigned to b_{595}, which is a rhombic high-spin heme. The intensity at g 5.94 is about 20 times larger than that at 5.55 under the conditions used here. So if the magnetic field is set at **g** = 5.94, the measured ENDOR signal will be the result of the *d* heme and the effect of b_{595} will be very small. When the magnetic field was set at **g** = 6.26, no ENDOR signal was observed under the same conditions used to measure line 5.94.

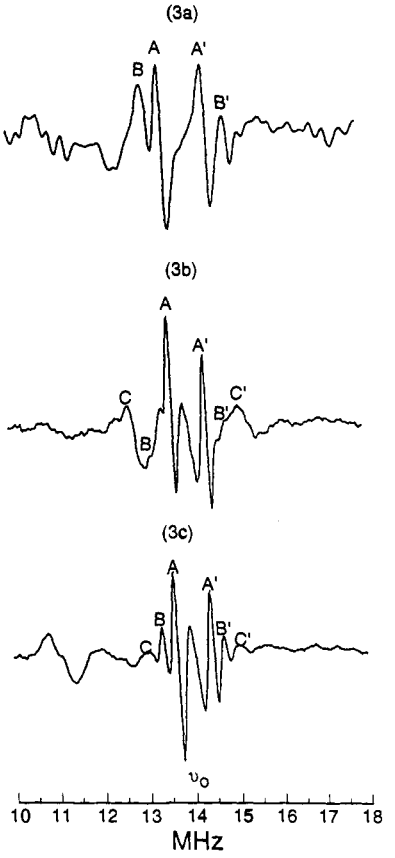

Figure 3. Proton ENDOR spectra at 7 K from the frozen solutions of cytochrome *d*, hemin, and metmyoglobin taken with the magnetic field along the heme normals, i.e., at **g** = 2.00. ENDOR were taken at radiofrequency power, 75 W; sweep range, 0.5–25.5 MHz; sweep time, 200 s; average of 10 scans; EPR microwave power, 15 mW; microwave frequency, 9.2807 GHz for cytochrome *d* (3a), 9.2700 GHz for hemin (3b), and 9.2645 GHz for metmyoglobin (3c). Frequency modulated, first-derivative presentation.

By use of $g_x = 6.26$ and $g_y = 5.55$, the g_z of b_{595} was calculated[15] to be 1.93. In this experimental spectrum, a line at $g = 1.93$ was observed. The intensity is only one-tenth that at $g = 2.00$ assigned to heme *d*. Line 1.93 does not show up well in Figure 2 because of its small signal intensity. For the same reason as above for the **g** = 5.94 line, the observed ENDOR signal at **g** = 2.00 is derived from the *d* heme and not from b_{595}; b_{558} is another *b*-type heme in the cytochrome *d* complex with a broad EPR line at g_z = 3.30. This low-spin EPR signal is difficult to visualize except in an expanded scale. The other small signals between **g** = 2 and **g** = 3 have been assigned to a small population of low-spin heme *d*, possibly caused by aging.[14] Only the axial signal assigned to the *d* heme was strong enough to obtain good ENDOR spectra.

Proton ENDOR from Cytochrome *d*, Hemin, and Metmyoglobin. Figure 3 shows the proton ENDOR spectra of cytochrome *d*, hemin, and metmyoglobin taken with the magnetic field along the heme normals, i.e., at a value corresponding to the **g** = 2.00 region. The best resolved proton hyperfine coupling constants for the three heme groups are summarized in Table I. For the proton spectrum of cytochrome *d* (Figure 3a), lines A and A′ have a hyperfine splitting of 0.9 MHz at the *z* direction, and B

(14) Meinhardt, S. W.; Gennis, R. B.; Ohnishi, T. *Biochim. Biophys. Acta* **1989**, *975*, 175–184.

(15) Lever, A. B. P.; Gray, H. B. In *Iron Porphyrins*; Addison-Wesley Publishing Company: Reading, MA, 1983; pp 43–88.

Table I. Proton Hyperfine Coupling Constants with the Magnetic Field along the Heme Normals (in MHz)[a]

	AA′	BB′	CC′
cytochrome *d*	0.90	1.80	
hemin	0.80		2.40
metmyoglobin	0.80	1.40	2.00

[a] The data were extracted from Figure 3.

and B′ have a splitting of 1.8 MHz. For the proton spectrum of hemin (Figure 3b), lines A and A′ show a hyperfine splitting of 0.80 MHz at the *z* direction, and C and C′ show a splitting of 2.4 MHz. The ENDOR spectrum obtained for metmyoglobin (Figure 3c) is similar to that seen by Mulks *et al.*,[16] except that the lines of heme-bound H_2O protons are not as intense. Mulks *et al.* have assigned A and A′ to the meso protons of the heme group and B and B′ to an exchangeable proton on the δ nitrogen of the proximal histidine. C and C′ were assigned to the two -CH protons of the histidine which are nearest the heme. In comparison, the A and A′ lines of all three compounds studied in this work are assigned to the meso protons. The proton from the proximal histidine seen in metmyoglobin was not seen in cytochrome *d* (compare Figures 3a and 3c, and see Table I for corresponding hyperfine coupling constants). ENDOR spectra of deuterated cytochrome *d* oxidase showed no change in lines in the proton frequency region (data not shown); therefore, the proton assigned to B and B′ is not exchangeable in cytochrome *d*.

N-14 ENDOR from Cytochrome *d*, Hemin, and Metmyoglobin. Figures 4a, 4b, and 4c compare the N-14 ENDOR spectra of cytochrome *d*, hemin, and metmyoglobin, respectively, with the magnetic field directed along the heme plane normals, i.e., with the magnetic field adjusted to $h\nu_{\text{microwave}}/2.00\beta_e$. All simulations were optimized with respect to peak positions, but ENDOR intensities were not explicitly considered because the calculations explicitly included neither level-to-level relaxation rates nor the differential rf ENDOR enhancement factor (see, for example, Geschwind[17]), effects which could account for the higher intensity of the two high-frequency peaks in Figures 4a and 4b. The simulated spectra are also displayed on the plots. If the canonical *z* directions from electron spin (q_z), nitrogen hyperfine coupling (A_z), and nitrogen quadrupole coupling (P_z) are parallel to each other, a single-crystal-like ENDOR spectrum should be seen. The experimental spectra from the three heme groups were of this kind. At this selected angle, a four-line ENDOR pattern from the heme plane nitrogen atoms of all three heme compounds is observed. This indicates that the four heme nitrogen atoms at this selected angle are essentially equivalent to each other. However, another four lines with larger nitrogen hyperfine coupling and nuclear quadrupole coupling than heme nitrogen atoms are obtained in the spectrum of metmyoglobin; they are generated by the nitrogen of histidine located at the axial direction of the heme plane. The ENDOR spectrum of cytochrome *d* was obtained at **g** equal to 2.00 and with microwave frequency equal to 9.2807 GHz. The ENDOR spectra of cytochrome *d* look much like the spectra of hemin with only four nitrogen lines at lower field, suggesting that cytochrome *d* most probably does not contain an axial nitrogen ligand.

During the simulation, the orientations of A_z and P_z of nitrogens were selected at the same heme direction as the g_z, with the sign of A_z being positive and the sign of P_z negative. Based on eq 5′ in the Appendix, if $P_z < 0$, the lower energy Zeeman pair, ν_N^-, will have a larger splitting than the upper pair, ν_N^+. From the experimental ENDOR spectra, the lower frequency N-14 Zeeman pairs indeed have a larger splitting than the higher frequency pair. The parameters from simulation are the most accurate at the field-selected *z* direction because of the single-crystal-like spectra. The errors are ±0.1 MHz for A_z and ±0.02 MHz for P_z.

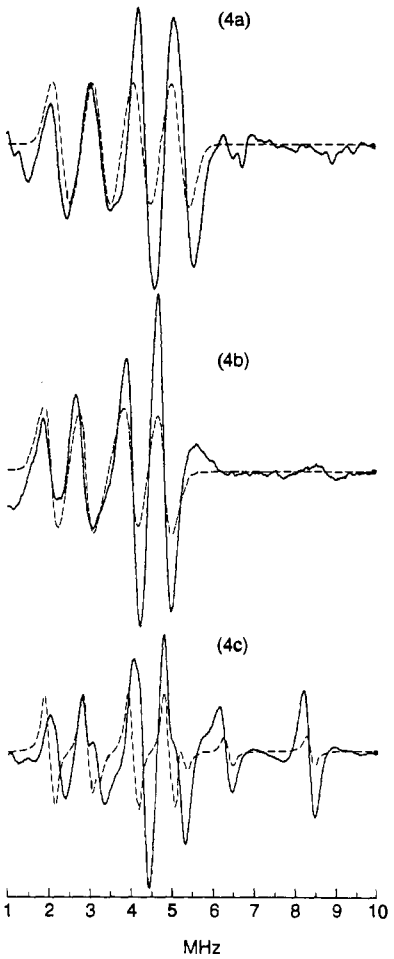

Figure 4. Nitrogen ENDOR spectra at 7 K from the frozen solutions of cytochrome *d*, hemin, and metmyoglobin with the magnetic field along the heme normals, i.e., at **g** = 2.00. The experimental conditions were the same as for Figure 3. (4a) Cytochrome *d*, (4b) hemin, and (4c) metmyoglobin. Also shown with dashed lines are the simulation spectra with the same ENDOR conditions as for the experiments for the three heme compounds. Intensities are not properly simulated (see text).

Figures 5a, 5b, and 5c show the experimental ENDOR spectra of cytochrome *d*, hemin, and metmyoglobin taken with the magnetic field in the heme plane, i.e., set at a value corresponding to **g** = 5.91. Figures 5a′, 5b′, and 5c′ show the simulated ENDOR spectra under the same conditions. All of A_x, A_y, P_x, and P_y in this region will make contributions to the ENDOR transition lines, and the observed spectra become complex. Scholes *et al.*[11] have reported that the four nitrogens in the heme plane are all different, but it is difficult to distinguish small differences among the four nitrogen atoms in these frozen solution samples. Therefore, during the simulation, only two sets of nitrogen hyperfine coupling and quadrupole coupling constants for the four nitrogen atoms, with different Euler angles (α, β, γ or θ_x, θ_y, θ_z) that describe the orientation differences between the **g** vector and the **A** vector, were assumed. By this approach, the simulated spectra could be fitted to the experimental spectra. As mentioned previously, the **g** matrix canonical coordinate system was chosen as the frame of reference for simulation. In order to fit the experimental data, the Euler angles θ_y and θ_z were set equal to 0. But in hemin, θ_x is equal to 22° for N_1, 112° for N_2, 202° for N_3, and 292° for N_4. In cytochrome *d*, θ_x = 25° for N_1, 115° for N_2, 205° for N_3, and 295° for N_4. In metmyoglobin the Euler angles of heme nitrogens are the same as for cytochrome

(16) Mulks, C. F.; Scholes, C. P.; Dickinson, L. C.; Lapidot, A. *J. Am. Chem. Soc.* **1979**, *101*, 1645–1654.
(17) Geschwind, S. In *Hyperfine Interactions*; Academic Press: New York, 1967; pp 235–239.

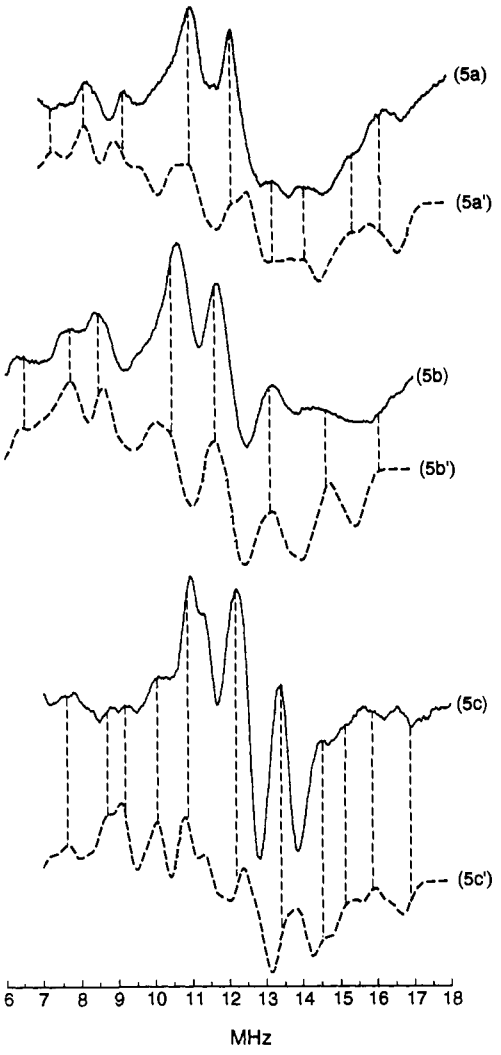

Figure 5. Nitrogen ENDOR spectra at 7 K from the frozen solutions of cytochrome *d*, hemin, and metmyoglobin with the magnetic field located at the heme planes, i.e., at **g** = 5.91. Other conditions for the ENDOR experiments were the same as in Figure 4. Spectra 5a, 5b, and 5c are the experimental spectra from cytochrome *d*, hemin, and metmyoglobin, respectively, and spectra 5a′, 5b′, and 5c′ are the simulated spectra with the same ENDOR conditions as the experiments for the three heme compounds, respectively. Intensities are not properly simulated (see text). Experimental spectra suffer from broadening and poor signal-to-noise ratios in some regions, but fit is judged by matching positions of reproducible features as closely as possible to positions of major simulated features, as indicated by dotted lines in the figure, and by general fit of overall shape.

d, although $\theta_x = 25°$ for the histidine nitrogen. In the **g** = 5.91 region, the errors in the parameters A_x and A_y are larger than the errors in A_z and P_z because the spectra are more complicated. All of the nitrogen hyperfine coupling and quadrupole coupling constants are summarized in Table II. From the table, one can see that the constants of hemin are smaller than those of cytochrome *d* and metmyoglobin and the constants of cytochrome *d* and metmyoglobin are close to each other. Although it is highly probable that cytochrome *d* does not have an axial nitrogen ligand, its heme pocket structure appears similar to that of metmyoglobin.

Discussion

In general, absolute orientations of **g**, **A**, and **P** cannot be determined by measurements on powder or frozen samples. Moreover, the quality of the powder-pattern ENDOR data limits the number of independent parameters which can be extracted by fitting peak position by simulations. Thus, we constrained all

Table II. Nitrogen Hyperfine Coupling and Nuclear Quadrupole Coupling Constants (in MHz) from Cytochrome *d*, Hemin, and Metmyoglobin[a]

	A_x	A_y	A_z	P_x	P_y	P_z
			Cytochrome *d*			
N_1	8.2	6.5	7.0	−0.97	1.30	−0.33
N_2	9.3	7.1	7.1	−1.01	1.33	−0.33
			Hemin			
N_1	7.7	6.1	6.8	−0.87	1.14	−0.29
N_2	8.6	6.7	6.7	−0.88	1.15	−0.29
			Metmyoglobin			
N_1	8.3	6.7	6.9	−0.92	1.22	−0.30
N_2	9.2	7.2	6.9	−0.93	1.23	−0.30
N_{his}	8.0	7.8	11.7	−0.26	1.31	−1.05

[a] The parameters were obtained from the best fit to the experimental spectra by using the NANGSEL program.

Table III. Distribution of Electron Spin Densities among the Ligand Nitrogen s and p Orbitals[a]

	f_s, %	$f_{p\sigma}$, %	$f_{p\pi}$, %
heme nitrogens of cytochrome *d*	2.3	1.8	0.6
heme nitrogens of hemin	2.3	1.9	1.7
heme nitrogens of metmyoglobin	2.3	2.2	0.3
histidine nitrogen of metmyoglobin	2.6	10	0.4

[a] The numbers given in the table were calculated on the basis of eq 6′, 7′, 9′, and 10′ in the Appendix and nitrogen hyperfine couplings obtained from the experiment.

canonical axis systems for a given nitrogen atom to be coincident. According to Scholes *et al.*,[11] the largest hyperfine coupling constants, A_x for heme nitrogens and A_z for the histidine nitrogen, are along the specific Fe–N bonds, with A_z perpendicular to the heme plane. The average Fermi contact contribution to the hyperfine coupling of the heme nitrogen is 7.6 MHz for cytochrome *d*, 7.1 MHz for hemin, 7.6 MHz for metmyoglobin, and 9.1 MHz for the histidine nitrogen of metmyoglobin. Therefore, the major part of the heme and histidine nitrogen hyperfine coupling is the Fermi contact interaction. The unpaired 2s electron densities of nitrogen were calculated by eq 6′ in the Appendix and are listed in Table III. The metmyoglobin parameters obtained here are close to those determined previously[11] by carefully oriented single-crystal measurements. The heme center in the single crystal may not be identical to that in a frozen solution, but one does not expect a great difference. It is gratifying that the frozen-solution ENDOR result is in such good agreement with the single-crystal result. One conclusion of this work is that the frozen-solution angle-selected ENDOR experiments, as interpreted by simulations, can provide a reasonable alternative to precise single-crystal rotation studies in cases where the single-crystal experiments are not feasible.

The nitrogen anisotropic hyperfine interaction has contributions from $p\sigma$ bonding to the iron $d_{x^2-y^2}$ and d_{z^2} orbital and from π bonding. With the use of eq 9′ and 10′ in the Appendix, and the values of A_d (0.47 MHz for the heme nitrogens of metmyoglobin and 0.41 MHz for the histidine nitrogen[11]), the unpaired electron densities in the $p\sigma$ and $p\pi$ orbitals, were computed. They are listed in Table III. The hyperfine interaction of Fe-57 in hemin has been measured to be 26.42 MHz, and the theoretical value is 27.9 MHz.[18] By comparing these values with the theoretically computed value for free ferric ion, −39.24 MHz,[19] one may estimate the unpaired electron density residing on the iron ion of hemin to be 68%. According to Koenig, the average bond length of Fe–N in chlorohemin is 2.007 Å with an angle β of 13.3°.[20] From eq 9′ in the Appendix and the data given for chlorohemin, the A_d of hydroxylhemin was calculated to be 0.467

(18) Mun, S. K.; Chang, J. C.; Das, T. P. *J. Am. Chem. Soc.* **1979**, *101*, 5562–5569.
(19) Ray, S. N.; Lee, T.; Das, T. P. *Phys. Rev. B Solid State* **1973**, *8*, 5291–5297.
(20) Koenig, D. *Acta Crystallogr.* **1965**, *18*, 663–673.

Table IV. Average Nitrogen Orbital Populations Estimated from Quadrupole Coupling Parameters[a]

	2θ, deg	a, in π orbital	b, in C–N bond	c, in lone pair	N_T, total nitrogen
Cytochrome *d*					
heme nitrogen	106	1.6	1.31	2.1	6.3
Hemin					
heme nitrogen	106.1	1.5	1.31	2.1	6.2
Metmyoglobin					
heme nitrogen	106	1.6	1.31	2.0	6.2
histidine nitrogen	109.6	1.6	1.33	2.0	6.2

[a] The numbers were estimated by using eq 11′ in the Appendix, experimentally obtained quadrupole coupling constants, and the assumed population of each of the two σ orbitals; $b = 1.31$ for the heme nitrogens and 1.33 for the histidine nitrogen.

Table V. Comparison between Theoretical and Experimental Values of Average Nitrogen Hyperfine and Nuclear Quadrupole Coupling Parameters (in MHz)

	A_x	A_y	A_z	A_{Fermi}	P_x	P_y	P_z	ref
				Cytochrome *d*				
heme (exptl)	8.8	6.8	7.1	7.6	−0.99	1.3	−0.33	this work
				Hemin				
heme (exptl)	8.2	6.4	6.8	7.1	−0.88	1.2	−0.29	this work
heme (theor)	8.99	2.50	3.80	5.10				26
				Metmyoglobin				
heme (exptl)	8.8	7.0	6.9	7.6	−0.93	1.2	−0.30	this work
heme (exptl)	9.86	6.89	7.1	7.95	−0.77	1.04	−0.27	11
heme (theor)	9.02	3.31	3.68	5.47	−1.10	1.79	−0.69	23
His (exptl)	8.4	7.0	11.7	9.0	−0.26	1.3	−1.05	this work
His (exptl)	8.0	7.8	11.6	9.1	−0.31	0.81	−1.12	11
His (theor)	2.70	2.70	8.18	4.53				23

MHz. The unpaired electron densities in the pσ and pπ orbitals of hydroxylhemin were obtained; these values are also shown in Table III. The f_{Fe} and R values are not available for cytochrome *d*. Since the nitrogen hyperfine coupling and quadrupole coupling values of cytochrome *d* are close to those of metmyoglobin and the direct dipole coupling constants, A_d, of hemin and metmyoglobin are very close to each other, it is reasonable to assume that the A_d of cytochrome *d* is 0.47 MHz. The calculated spin densities on the pσ and pπ orbitals for the nitrogens of cytochrome *d* are also shown in Table III. For an sp^2 orbital scheme, the ratio of f_p to f_s in the pσ bond would be 1. The ratio determined here is about 1.1 for the heme nitrogens of metmyoglobin; Scholes *et al.* reported a ratio of 2. We believe that the difference is well within the combined experimental errors.

From eqs 11′ in the Appendix and the nitrogen quadrupole coupling constants, the electron population in each orbital of the nitrogen atoms could be estimated. However, the **P** tensor is traceless, i.e., only two of three principal parameters are independent. In order to obtain the populations *a*, *b*, and *c*, one of them has to be known or arbitrarily set. The population of each of the two σ orbitals, *b*, was chosen as 1.31 for the heme nitrogen and 1.33 for the histidine nitrogen.[11,21,22] The C–N–C angles are 106° for the heme nitrogens of metmyoglobin and cytochrome *d*, 106.1° for the heme nitrogens of hemin, and 109.6° for the histidine nitrogen of metmyoglobin.[11,20] The nitrogen orbital populations from quadrupole data were computed and are listed in Table IV.

Comparisons of our experimental data with theoretical values are summarized in Table V. As pointed out by Das and coworkers,[23] the agreement between theoretical and experimental data in a number of heme systems exists only in trends, and the absolute values of the theoretical results can be up to 50% lower than the experimental values. Our data on hemin and metmyoglobin compare well with other experimental data in this respect.

Conclusions

1. Our ENDOR spectra of frozen solutions of cytochrome *d* and of hemin, which has no axial nitrogeneous ligand, display similar features, while frozen-solution ENDOR of metmyoglobin, known to have a ligated histidine, displays extra features attributable to an axial nitrogen.

2. From our ENDOR data on cytochrome *d*, we conclude that the axial ligand to the *d* heme is most probably not a histidine or other strong nitrogenous ligand. Electron paramagnetic resonance studies of the NO-bound form of cytochrome *d* support this conclusion (unpublished data in this laboratory). Therefore, it appears that the histidine at position 19 of the oxidase is not a ligand to the *d* heme but may act as a ligand to b_{595}. Additional mutagenesis and spectroscopic techniques are being used to determine the remaining unknown axial ligands.

3. Useful ENDOR spectra of metalloproteins in frozen solution are obtained at a range of magnetic field strengths corresponding to different molecular orientations and can be interpreted through simulation with our program NANGSEL.

4. Comparison of metmyoglobin ENDOR so obtained and interpreted with single-crystal auqometmyoglobin ENDOR previously reported shows good agreement in the electronic Zeeman, hyperfine, and nuclear quadrupole coupling matrices. This agreement demonstrates that angle-selected ENDOR of frozen solutions of metalloproteins, acquired over a wide range of magnetic field and analyzed by simulation, can be a useful, although not complete, alternative to for orientation-dependent single-crystal ENDOR studies. That is, a substantial amount of the same information can be obtained with less experimental difficulty.

Acknowledgments. We thank Professor Charles P. Scholes (SUNY at Albany) for illuminating discussion and for providing auxiliary material for ref 11, Professor Peter G. Debrunner (University of Illinois) and Marvin M. Makinen (The University of Chicago) for cooperation in accomplishing some of the ENDOR spectroscopy, and Professor P. D. Morse II (Illinois State University and Scientific Software Systems) for adapting the EW software system for ENDOR spectrometer control. Facilities of the Illinois EPR Research Center, a national Research Resource funded by the National Institutes of Health (Division of Research Resources, RR01811), were used in this work. The NANGSEL program was developed under the auspices of both RR01811 and the Biotechnology Resource in Pulsed EPR Spectroscopy at Albert Einstein College of Medicine in The Bronx, NY, funded by the National Institutes of Health, Grant RR02583. Research funding was provided by NIH Grants GM42208 and HL16101 and by the donors of the Petroleum Research Fund, administered by the American Chemical Society.

Appendix

Proton Hyperfine Coupling. The proton hyperfine coupling constants may be written

$$A_{LH} = a_H + A_{dH}$$

a_H is the Fermi contact interaction[25]

$$a_H = (^2/_3h)\pi g g_H \beta_e \beta_H |1s_H(0)|^2 \rho_H \qquad (1')$$

where $|1s_H(0)|^2$ is the probability of the electron in a hydrogen orbital at the proton and ρ_H is the unpaired spin density on the proton. In fact, $a_H = a_0\rho_H$, where a_0, 1422.74 MHz, is the Fermi

(21) Hsieh, Y. N.; Rubenacker, G. V.; Cheng, C. P.; Brown, T. L. *J. Am. Chem. Soc.* **1977**, *99*, 1384–1389.
(22) Lucken, E. A. C. In *Nuclear Quadrupole Coupling Constants*; Academic Press: New York, 1969; pp 79–96.
(23) Han, P. S.; Das, T. P.; Rettig, M. F. *Theor. Chim. Acta (Berlin)* **1970**, *16*, 1–21.
(24) Timkovich, R.; Cork, M. S.; Gennis, R. B.; Johnson, P. Y. *J. Am. Chem. Soc.* **1985**, *107*, 6069–6075.
(25) Brown, T. G.; Hoffman, B. M. *Mol. Phys.* **1980**, *39*, 1073–1109.

hyperfine coupling constant for a hydrogen atom. A_{dH} represents the anisotropic part of the proton hyperfine coupling matrix. If one assumes that the electron is a point dipole located on the metal ion and uses the canonical **g**-tensor coordinate system of the **g** matrix, the explicit expression for A_{dH} in frequency units is[8]

$$A_{ij} = -\beta_e g_N \beta_N g_i (3\hat{\mathbf{r}}_i \hat{\mathbf{r}}_j - \delta_{ij})/(hR^3) \qquad (2')$$

where i or j represents axis x, y, or z, and R is the distance from the center metal ion to the proton. If θ_H and ϕ_H are the coordinates of the proton in the polar coordinate system, then $\hat{\mathbf{r}}_x = \cos\phi_H \sin\theta_H$, $\hat{\mathbf{r}}_y = \sin\phi_H \sin\theta_H$, and $\hat{\mathbf{r}}_z = \cos\theta_H$. An expression for the frequency of a proton ENDOR transition in a powder sample is[8]

$$\nu_H = \{\sum_{i=1}^{3}[m_s(\sum_{j=1}^{3} g_j h_j A_{ji})/(g(\theta,\phi)) - h_i \nu_0]^2\}^{1/2}$$

where $\nu_0 = g_N\beta_N B/h$, θ and ϕ are the coordinates of the applied magnetic field in the polar coordinate system, $h_x = \cos\phi \sin\theta$, $h_y = \sin\phi \sin\theta$, and $h_z = \cos\theta$. If the applied magnetic field is parallel to the g_z and A_z directions and perpendicular to the g_x and g_y directions, the expression for the frequency of the ENDOR transitions is

$$\nu_H = |\nu_0 \pm {}^1/_2 A_z| \qquad (3')$$

N-14 Hyperfine Coupling. N-14 does not show the same kind of ENDOR pattern as protons because the nuclear spin of N-14 is 1 and the nuclear quadrupole coupling must be taken into account. Taking the magnetic field **B** along the heme normal (z axis), one obtains to first order four ENDOR frequencies at

$$\nu_N = {}^1/_2|A_z| \pm \nu_{N_0} \pm {}^3/_2 P_z \qquad (4')$$

and to second order one obtains[11]

$$\nu_N^+ = {}^1/_2|A_z| + (P_x - P_y)^2/[4(A_z \pm 2\nu_{N_0})] - {}^3/_2 P_z \pm [\nu_{N_0} - 9(A_x - A_y)^2/(8\nu_e)] \qquad (5a')$$

$$\nu_N^- = {}^1/_2|A_z| + (P_x - P_y)^2/[4(A_z \pm 2\nu_{N_0})] + {}^3/_2 P_z \pm [\nu_{N_0} + 9(A_x + A_y)^2/(8\nu_e)] \qquad (5b')$$

where A_x, A_y, and A_z are the nitrogen hyperfine coupling constants, P_x, P_y, and P_z are the N-14 nuclear quadrupole coupling constants, ν_N is the Larmor frequency (the Zeeman term) of the N-14 in the applied magnetic field, and ν_e is the applied microwave frequency.

It is customary to write the Fermi contact interaction due to unpaired spin density in the nitrogen 2s orbital as[25-27]

$$A_{Fermi} = (8 \times 10^{-6}) f_s \beta_e \beta_N |\Psi_{2s}(0)|^2 \pi/(3hS) \qquad (6')$$

where f_s is the fraction of an unpaired electron in a 2s orbital, $\Psi_{2s}(0)$ is the 2s wave function of the nitrogen at the N nucleus, S equals ${}^5/_2$, and $|\Psi_{2s}(0)|^2$ equals 33.4×10^{24} cm^{-3}. The anisotropic part of the nitrogen hyperfine coupling may be divided into two portions, A_p and A_d. The former is related to the unpaired electron density on nitrogen, and the latter is the contribution by the direct dipolar coupling to the central iron electron spin density. A_p and A_d are defined as

$$A_p = 10^{-6} f_p g g_N \beta_e \beta_N \langle 1/r^3 \rangle_{2p}/(5hS) \qquad (7')$$

$$A_d = 10^{-6} f_{Fe} g g_N \beta_e \beta_N/(hR^3) \qquad (8')$$

where f_p and f_{Fe} are the fractions of an unpaired electron in a particular p orbital and the fraction of the total spin residing on the central iron ion, respectively. Here, $\langle 1/r^3 \rangle_{2p} = 2.1 \times 10^{24}$ cm^{-3}, which is the expectation value of $1/r^3$ for a nitrogen p electron, and R is the Fe–N distance. So the total A_{ij} for the heme nitrogens is[11]

$$A_x = A_{Fermi} + (3\cos^2\beta - 1)A_d + 2A_\sigma - A_\pi \qquad (9a')$$

$$A_y = A_{Fermi} - A_d - A_\sigma - A_\pi \qquad (9b')$$

$$A_z = A_{Fermi} - (1 - 3\sin^2\beta)A_d - A_\sigma + 2A_\pi \qquad (9c')$$

$$A_{xz} = {}^3/_2(\sin(2\beta))A_d \qquad (9d')$$

and for the histidine nitrogen is

$$A_x = A_{Fermi} - A_d - A_\sigma + 2A_\pi \qquad (10a')$$

$$A_y = A_{Fermi} - A_d - A_\sigma - A_\pi \qquad (10b')$$

$$A_z = A_{Fermi} + 2A_d + 2A_\sigma - A_\pi \qquad (10c')$$

where A_σ is the dipolar interaction with an unpaired electron in a nitrogen p_σ orbital, A_π is the dipolar interaction with an unpaired electron in the nitrogen p_π orbital perpendicular to either the pyrrole ring of the heme or to the imidazole ring of the histidine, and β is the out-of-planarity angle.[28] A_p is the sum of A_σ and A_π.

To understand the nuclear electric quadrupole coupling parameters, the model originally proposed by Townes and Dailey (TD)[29] is useful; moreover, the results of a TD analysis here are readily compared to a similar analysis in the literature.[11] The principal elements of the quadrupole tensor, P_x, P_y, and P_z, for the heme nitrogens are[21]

$$P_x/P_0 = c(1 - \cot^2\theta) + b(\cot^2\theta - {}^1/_2) - a/2 \qquad (11a')$$

$$P_y/P_0 = -c/2(1 - \cot^2\theta) + b/2(2 - \cot^2\theta) - a/2 \qquad (11b')$$

$$P_z/P_0 = -c/2(1 - \cot^2\theta) - b/2(1 + \cot^2\theta) + a \qquad (11c')$$

where P_x, P_y, and P_z are associated with directions along the Fe–N bond, perpendicular to the Fe–N bond, and along the π bond perpendicular to the heterocycle, respectively. The out-of-plane nitrogen $p\pi$ orbital is assigned a population a, and each of the two σ orbitals is assigned a population b. The lone-pair orbital is assigned a population c. The angle θ is half of the C–N–C angle, and $P_0 = {}^1/_2\, e^2Qq_0/h = -4.5$ MHz.[21,22] For the histidine nitrogen, the subscripts z and x should be interchanged.

(26) Maki, A. H.; McGarvey, B. R. *J. Chem. Phys.* **1958**, *29*, 35–38.
(27) Hartree, D. R.; Hartree, W. *Proc. R. Soc. London Ser. A.* **1948**, *193*, 299–304.
(28) Takano, T. *J. Mol. Biol.* **1977**, *110*, 537–568.
(29) Townes, C. H.; Dailey, B. P. *J. Chem. Phys.* **1949**, *17*, 782–796.